

# Toward 3D-TRUS image-guided interstitial brachytherapy for cervical cancer

Johannes Knoth<sup>1</sup>, Nicole Nesvacil<sup>1</sup>, Alina Sturdza<sup>1</sup>, Gernot Kronreif<sup>2</sup>, Joachim Widder<sup>1</sup>,  
Christian Kirisits<sup>1</sup>, Maximilian Paul Schmid<sup>1,\*</sup>

<sup>1</sup>Department of Radiation Oncology, Comprehensive Cancer Center, Medical University of Vienna, Vienna, Austria

<sup>2</sup>Austrian Center for Medical Innovation and Technology, Wr. Neustadt, Austria

## ABSTRACT

**PURPOSE:** To qualitatively and quantitatively analyze needle visibility in combined intracavitary and interstitial cervical cancer brachytherapy on 3D transrectal ultrasound (TRUS) in comparison to gold standard MRI.

**METHODS AND MATERIALS:** Image acquisition was done with a customized TRUS stepper unit and software (Medcom, Germany; Elekta, Sweden; ACMIT, Austria) followed by an MRI on the same day with the applicator in place. Qualitative assessment was done with following scoring system: 0=no visibility 1 (= poor), 2 (= fair), 3 (= excellent) discrimination, quantitative assessment was done by measuring the distance between each needle and the tandem two centimeters (cm) above the ring and comparing to the respective measurement on MRI.

**RESULTS:** Twenty-nine implants and a total of 188 needles (132 straight, 35 oblique, 21 free-hand) were available. Overall, 79% were visible (87% straight, 51% oblique, 76% free-hand). Mean visibility score was  $1.4 \pm 0.5$  for all visible needles. Distance of the visible needles to tandem was mean  $\pm$  standard deviation (SD) 21.3 millimeters (mm)  $\pm$  6.5 mm on MRI and 21.0 mm  $\pm$  6.4 mm on TRUS, respectively. Difference between MRI and TRUS was max 14 mm, mean  $\pm$  SD -0.3 mm  $\pm$  2.6 mm. 11% differed more than 3 mm.

**CONCLUSIONS:** Straight needles were better detectable than oblique needles (87% vs. 51%). Detectability was impaired by insufficient rotation of the TRUS probe, poor image quality or anatomic variation. As needles show a rather indistinct signal on TRUS, online detection with a standardized imaging protocol in combination with tracking should be investigated, aiming at the development of real time image guidance and online treatment planning. © 2021 The Authors. Published by Elsevier Inc. on behalf of American Brachytherapy Society. This is an open access article under the CC BY license (<http://creativecommons.org/licenses/by/4.0/>)

## Keywords:

Cervical cancer; Image guidance; Trus and/or interstitial brachytherapy

## Introduction

The evolving role of MRI-based image-guided adaptive brachytherapy with a combined intracavitary and/or interstitial approach as part of primary radiochemotherapy for advanced cervical cancer led to major improvements in treatment outcome (1). The distinct tumor visi-

bility on MRI allows for precise placement of interstitial needles, thereby enabling a therapy adapted to the actual tumor dimensions respecting the surrounding organs at risk (OARs).

Nevertheless, MRI-based treatment planning comprises some disadvantages such as difficult logistics, time consuming image acquisition, comparably high costs, and the missing opportunity for real time guidance during interstitial needle insertion. In addition, needle positions have to be planned before the procedure with the aid of MRI images, while needles are inserted in a “blind” manner and positions are checked only afterwards (again on MRI), entailing the risk of highly time- and resource-consuming repeat procedures in case of suboptimal needle placement.

Received 22 July 2021; received in revised form 13 October 2021; accepted 19 October 2021

\* Corresponding author. Department of Radiation Oncology, Comprehensive Cancer Center, Medical University of Vienna, General Hospital of Vienna, Währinger Gürtel 18-20, A-1090 Vienna, Austria, Tel.: +4314040026920; fax: +4314040026930

E-mail address: [maximilian.schmid@akhwien.at](mailto:maximilian.schmid@akhwien.at) (M.P. Schmid).

Interventional MRI as a possible alternative is limited to very few institutions and still requires scanning time and patient movement between scans.

Transrectal ultrasound (TRUS) is a well-established imaging modality in prostate cancer treatment planning and is routinely used there for real time needle guidance. Treatment-relevant assessment of tumor dimensions in gynecology is non-inferior to MRI (2,3,4) and the interobserver variability in regard to target delineation on TRUS is comparable (5). A combination of CT (for the depiction of OARs) and TRUS (for target delineation) (6) might therefore overcome the need for MRI in image-guided adaptive brachytherapy (IGABT) planning and could thereby facilitate the entire procedure in terms of logistics, time and cost, but also in terms of real time needle guidance in the operating room. By immediate feedback during the insertion process, real time needle guidance could improve the geometry of the implant, and subsequently improve target coverage. To further develop TRUS in the direction of real time needle guidance, assessment of needle visibility and precise knowledge of the spatial relation of interstitial needles to the tandem are necessary. Therefore, we qualitatively and quantitatively analyzed the visibility and position of interstitial needles on TRUS at the time of brachytherapy with applicator in place in comparison to MRI.

## Material & methods

### *Patients and treatment*

This study comprised image data sets from two previous prospective trials on 3D-TRUS in cervical cancer brachytherapy conducted between 09/2012–05/2013 (4) and 10/2015–09/2016 (5). Patients with FIGO IB to IVB (para-aortic nodes only) undergoing primary chemoradiotherapy were eligible. All patients provided written consent. Treatment consisted of pelvic external beam radiotherapy (45–50.4 Gy in 25–28 fractions) with or without concomitant chemotherapy (Cisplatin 40 mg/m<sup>2</sup> for five cycles) followed by IGABT. The latter was performed at the end of the treatment over four fractions administered within two applications delivering a total dose of >85 Gy EQD2 (equieffective dose, reference dose 2 Gy per fraction, linear quadratic model,  $\alpha/\beta = 10$  Gy) to the D90 of the high-risk clinical target volume (HR-CTV). Tandem-ring applicators (“Vienna”-type, Elekta, Sweden) with interstitial titanium needles were used for dose delivery. Interstitial needles could be inserted through predefined holes in the ring of the applicator in a straight and/or oblique manner as well as “free-hand” without fixation to the applicator. Straight insertion is defined as parallel to the tandem in the axis of the uterus. Oblique insertion is defined as diagonally from the ring directed to the parametrial tissue with an angle of 20° to the tandem. “Free-hand” needles were typically implanted either anterior of the ring peri-

urethrally or lateral of the ring into the middle and/or distal parametrium for regions not reachable with predefined needle positions.

Inclusion criteria were completion of TRUS and MRI with the applicator in place on the same day.

### *TRUS*

3D-TRUS image acquisition was always done by the same investigator (MS) with a customized TRUS stepper device and software (Medcom, Germany; Elekta, Sweden; ACMIT, Austria). The examination was performed under anesthesia in lithotomy position with the applicator in place after bowel preparation and bladder filling according to a dedicated in-house standard protocol. After manual insertion according to the position and flexure of the uterus and/or applicator, the TRUS probe (BIOPSEE, Medcom, Germany) was connected, and fixated to a customized ultrasound stepper unit. In the first trial (4), images were acquired by a dedicated registration software during a manual pull-back of the TRUS probe. In the second trial (5), images were acquired during an automated rotation of the TRUS probe along its longitudinal axis.

### *MRI*

MRI in the first series (4) was performed with a 1.5 Tesla system (Avanto, Siemens AG, Germany), MRI in the second series (5) was performed with a 0.35 Tesla system (Magnetom C, Siemens AG, Germany) according to the Gyn GEC ESTRO recommendations for imaging in IGABT (7). In both series (4,5), T2-weighted axial, and para-axial images were obtained covering the area from the tip of the uterine fundus to the caudal border of the pubic symphysis including any vaginal tumor extension with the applicator in place. Slice thickness in both series was 5 mm.

### *Image analysis*

The main objective of this study was assessment of quantitative and qualitative needle visibility on TRUS images in comparison to MRI. For optimal comparability, all image data sets were evaluated in transverse view in the axis of the uterus on a predefined slice level 2 cm above the ring (at the level of point A, see also Fig. 1). The following methodology was applied: Sagittal images (Fig. 2) were used to identify the ring and tandem as landmarks of the applicator. A distance of 2 cm was then measured along the tandem, to reach the respective slice level. At this level, transverse images were analyzed in regard to (1) needle visibility (yes vs. no), (2) distance of each needle to the tandem in mm and (3) qualitative visibility, which was scored as follows: 0 = no visibility, 1 = poor discrimination, edge of needle blurred, 2 = fair discrimination, edge of needle indistinct, 3 = excellent discrimination, edge of needle

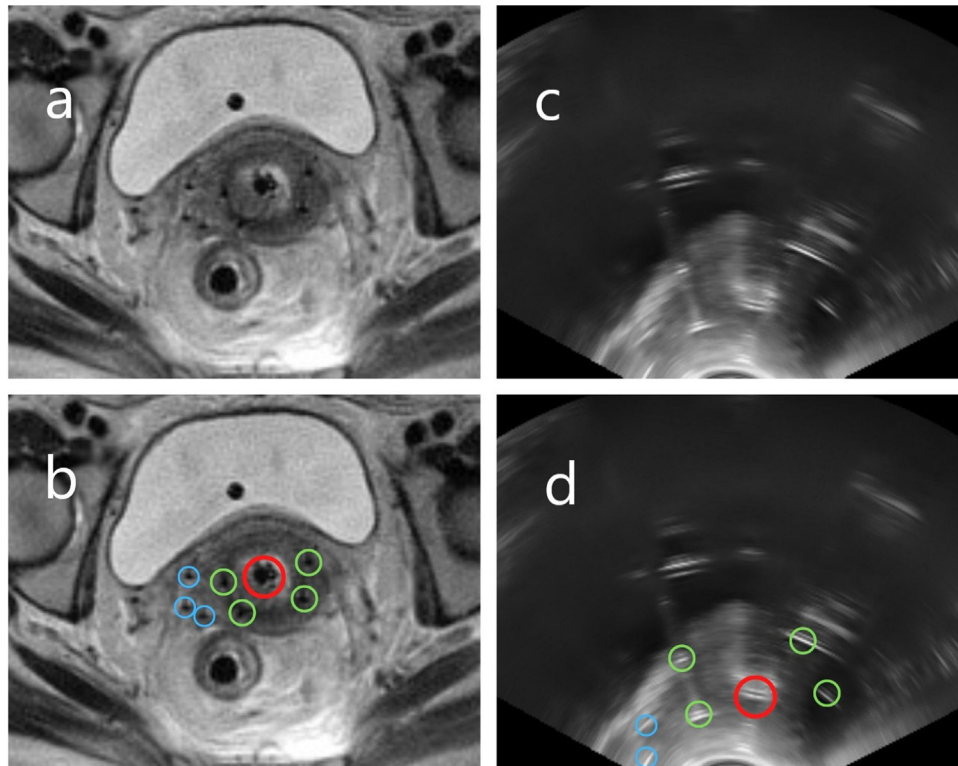


Fig. 1. (a) Transversal MRI image at the level of point A (2 cm above the ring). (b) Tandem (red), straight needles (green) and oblique needles (blue) marked on MRI. (c) Transversal TRUS image at the level of point A (2 cm above the ring) of the same patient. (d) Tandem (red), straight needles (green) and oblique needles (blue) marked on TRUS. In comparison to MRI, the most lateral oblique needle is outside the field of view (FOV). (For interpretation of the references to color in this figure legend, the reader is referred to the web version of this article.) (Color version of the figure is available online.)

distinct. Written reports of the applicator insertion were provided to understand the applicator geometry including applicator type, size and number of implanted needles, direction and depth of insertion. Each available needle position was systematically labelled for exact identification and subsequent comparison.

Image analysis was performed by one investigator (JK) to avoid interobserver variability. To reduce a potential bias, all TRUS images were evaluated first. MRI images were not viewed until after the ultrasound assessment was completed. To test for intraobserver variability, measurements of three randomly chosen patients were taken twice a few days apart.

#### Statistical analysis

Descriptive statistics using Excel 2016 (Microsoft, USA) were done to calculate maximum (max), minimum (min), median, mean  $\pm$  standard deviation (SD) for distance and visibility score for all needles as well as for straight, oblique and free-hand needles separately. Paired *t* tests using SPSS Statistics (Version 24, IBM, USA) were performed to test for significant differences between MRI and TRUS. Fisher exact test was used to compare the vis-

ibility (yes vs. no) of straight, oblique, and free-hand needles.

## Results

#### Patients and application

Forty-eight patients were considered for this study, and 24 were excluded due to solely intracavitary implants ( $n=19$ ) and/or incomplete TRUS data ( $n=6$ ). In total, 24 patients with FIGO Stage IB3-IIIb with 29 applications and a total of 188 needles (132 straight through the ring, 35 oblique through the ring, and 21 “free-hand”) were available for analysis.

#### Qualitative analysis

On TRUS, tandem and ring were visible in every patient. Overall, 149/188 needles (79.3%) were visible. The visibility of straight (87.1%), oblique (51.4%) and free-hand (76.2%) needles varied significantly ( $p < 0.001$ ). The mean visibility score was  $1.4 \pm 0.5$  SD for all visible needles on TRUS. The difference in mean visibility between patients from the first trial (4) ( $1.41 \pm 0.54$ ) and the second trial (5) ( $1.43 \pm 0.53$ ) was not significant ( $p=0.85$ ).

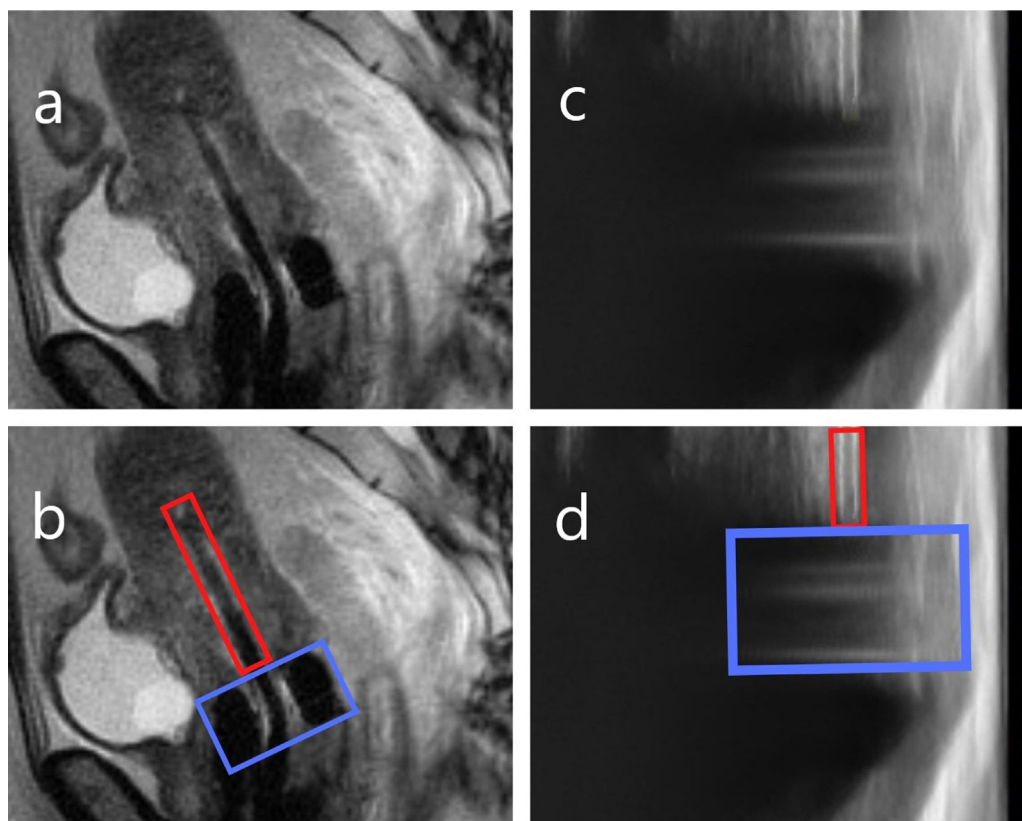


Fig. 2. Sagittal MRI image with applicator in place. Tandem (red) and ring (blue) marked on MRI. Sagittal TRUS image of the same patient with the applicator in place. Tandem (red) and ring (blue) marked on TRUS. (For interpretation of the references to color in this figure legend, the reader is referred to the web version of this article.) (Color version of the figure is available online.)

Table 1

All non-detectable needles allocated to route of insertion (top line) and reason for non-detectability (left column) in total numbers and percent. (FOV = field of view)

	Straight needles (n = 132)	Oblique needles (n = 35)	“Free-hand” needles (n = 21)	Total (n = 188)
Not visible inside FOV	2/132 (1.5%)	8/35 (22.9%)	2/21 (9.5%)	12/188 (6.4%)
Outside FOV	6/132 (4.6%)	3/35 (8.6%)	0/21 (0.0%)	9/188 (4.8%)
Masked by myoma (one patient)	5/132 (3.8%)	4/35 (11.4%)	2/21 (9.5%)	11/188 (5.9%)
TRUS probe inserted <2 cm above the ring (one patient)	4/132 (3.0%)	2/35 (5.7%)	1/21 (4.8%)	7/188 (3.7%)
Total	17/132 (12.9%)	17/35 (48.6%)	5/21 (23.8%)	39/188 (20.7%)

Characteristics for the non-detectable needles are summarized in Table 1.

### Quantitative analysis

Distance of the visible needles to tandem was max 51 mm, min 8 mm, mean ± SD 21.3 mm ± 6.5 mm on MRI and 49 mm, 10 mm, 21.0 mm ± 6.4 mm on TRUS, respectively. Difference in needle-to-tandem distance between MRI and TRUS was max 14 mm, mean ± SD -0.3 mm ± 2.6 mm, which was not significant (p = 0.20) There was also no significant difference regarding straight (p = 0.66), oblique (p = 0.11) and “free-hand”

needles (p = 0.38) alone. The respective results can be found in Table 2. 16/149 needles (10.7%) had a difference of more than 3 mm.

Max and mean ± SD intraobserver variability was 2 mm and -0.1 mm ± 1.0 mm on MRI and 2 mm and 0.3 mm ± 1.1 mm on TRUS, respectively.

### Discussion

In this study, differences in needle visualization between TRUS and MRI in the treatment of locally advanced cervical cancer with IGABT (utilizing a ring / tandem – “Vienna-type” - applicator) as part of concomitant radio-



Table 2

Max, min, median, mean  $\pm$  SD for (1) visibility score, (2) distance to tandem in millimeter on TRUS 2 cm above the ring, (3) distance to tandem in millimeter on MRI 2 cm above the ring and (4) difference between TRUS and MRI in millimeter 2 cm above the ring, displayed for all visible needles as well as for visible straight, oblique and “free-hand” needles separately

		Max	Min	Median	Mean	SD
All needles (n = 149)	Visibility	3	1	1	1.4	0.5
	TRUS	49	10	19	21.0	6.4
	MRI	51	8	19	21.1	6.4
	Difference	7	–14	0	–0.14	2.33
Straight needles (n = 115)	Visibility	3	1	1	1.5	0.6
	TRUS	25	10	19	18.6	2.6
	MRI	25	8	19	18.7	2.5
	Difference	4	–14	0	–0.1	2.1
Oblique needles (n = 18)	Visibility	2	1	1	1.1	0.3
	TRUS	38	23	32	31.2	4.5
	MRI	36	25	33	32.4	3.0
	Difference	5	–5	–2	–1.3	3.0
“Free-hand” needles (n = 16)	Visibility	2	1	1	1.3	0.44
	TRUS	49	11	27.5	27.6	11.3
	MRI	51	10	25.5	27.0	11.0
	Difference	7	–4	0.5	0.6	2.8

chemotherapy were retrospectively evaluated. The study showed that needles were well identifiable on TRUS overall, but with significant differences depending on the insertion direction. Oblique needles, employed to cover the middle to distal parametrium, were only visible in 51% of the cases. In contrast, straight needles, which represent the largest group of interstitial needles in terms of needle orientation in combined intracavitary / interstitial brachytherapy of cervical cancer, were detectable in 87%. This might be explained - besides the shorter distance to the ultrasound probe - by the easier needle distinction. Straight needles are usually located inside the cervix and/or tumor, which typically has a dark signal allowing for clear differentiation of the bright signal of the titanium needle. Oblique needles, however - if not placed inside the tumor - are located within the parametrial space, resembling the bright signal of the needles. Although 79% of the needles were visible, the image quality of the visible needles was relatively low with a mean score of 1.4, indicating poor to fair discrimination with indistinct edges of needles. This finding was not surprising as titanium was used as needle material, which induces ultrasound artefacts. However, despite the low image quality, quantitative analysis revealed a surprisingly high correlation to the MRI reference with a mean difference of 0.3 mm and a standard deviation of 2.6 mm. Eighty-nine percent of all visible needles were displayed within a difference of 3 mm. One needle had a difference of 14 mm. This was observed in a patient with in total 12 inserted needles. Poor discrimination due to surrounding artefacts and acoustic shadowing might be the underlying reason for this relatively large difference. Similar to our study, Rodgers *et al.* recently reported that 78% of needles had a point difference of less than 3 mm comparing CT and transvaginal ultrasound (TVUS) in patients with vaginal malignancies. However, in that study

all needles had been visible (8). The higher rate of visibility in comparison to our study might be related to the anatomically more distal (and thus better reachable) location of the vagina in comparison to the cervix. Another paper of the same group comparing TRUS to CT resulted in a needle visibility of 88%. Reasons for non-visibility were mainly applicator-related (cylinder type) (9). In our study, reasons for non-visibility were anatomic variation (in one patient), needles placed outside the FOV of the 3D-volume, artefacts, and inadequate insertion depth of the TRUS probe (in one patient). Optimized needle material specifically developed for TRUS and standardized imaging protocols should be considered for future studies to improve detectability.

Another group investigated the relation of interstitial needles to the cervix in cervical cancer patients treated with an ovoid-shaped - “Utrecht-type” - applicator (Elekta, Sweden; insertion angle 15°–25°) on TRUS in comparison to MRI. Distances on transverse images were measured directly above the ovoids from the needle to the left, right, anterior and posterior surface of the cervix. Apparently, all needles were visible at this level. Distances between MRI and TRUS did not differ significantly and the interclass correlation coefficient was >0.9 in all four directions (10). In agreement, we did not observe significant differences (even with using the level of point A as reference level) in our cohort using tandem-ring applicators.

The current findings from our study and the recent literature underline the evolving role of TRUS in cervical cancer brachytherapy. The observation that - if a needle is identified on TRUS - the spatial location in relation to the tandem and cervix is representative of the subsequent MRI opens the room for further exploration of real-time needle guidance. The advantage of such an approach is the possibility to guide, evaluate and confirm the needle position

before transferring the patient to MRI and by that optimize the implant quality. In our institution, currently, all patients undergo dynamic free-hand standard TRUS (without dedicated technology described in this study) during and at the end of applicator and needle placement as routine procedure. A scientific evaluation of this simpler technique is challenging, but clinical experiences are promising. The above-mentioned limitations in visibility and image quality, however, remain and impede further developments in the direction of TRUS needle reconstruction and online treatment planning. Needle tracking with optical or electromagnetic tracking (EMT) might be an interesting option to overcome these limitations. In prostate cancer brachytherapy, EMT was introduced to improve detectability of needles as well as accuracy and verification of needle reconstruction. A phantom test investigating the needle tip difference between EMT and CT with micro-CT as gold standard resulted in a tip detection error of  $0.7 \text{ mm} \pm 0.3 \text{ mm}$  with EMT and  $1.1 \text{ mm} \pm 0.7 \text{ mm}$  with CT (11). Another pelvic phantom test comparing EMT trajectories to TRUS trajectories showed a coordinate difference of  $1.3 \text{ mm} \pm 0.3 \text{ mm}$  and an angle difference of  $1.6^\circ \pm 0.3^\circ$  (12). Using TRUS alone, a mean needle localization error of 1.7 mm with a needle detection rate of 85% was achieved, compared to 3.7 mm and 100% with EMT alone. Combining TRUS and EMT resulted in a mean needle localization error of 1.8 mm and a needle detection rate of 100% (13). Given a comprehensive calibration workflow, localization accuracy of  $<1 \text{ mm}$  can be achieved with EMT (14). This accuracy within 30 cm distance of a typical tracking device is not impaired by commonly used prostate brachytherapy devices. Only a metal arm at a distance of 10 cm to the sensor might cause a mean absolute error of 1.4 mm (15). These findings cumulated in a workflow describing a real-time EMT-tracking based, 3D-TRUS treatment platform (16), which might offer some resulting research questions for gynecologic brachytherapy applications to be addressed in future studies. The combination of TRUS with EMT in cervical cancer brachytherapy could help overcome the impaired spatial resolution of interstitial needles on TRUS and might offer a tool to detect non-visible needles. Besides the possibility to verify needle reconstruction, the latter would generally be simplified, and the development of an online treatment planning workflow (to see a live dose calculation already in the operating room) would be facilitated. Fusing a TRUS- and EMT-based treatment plan with CT images (for organ at risk definition) could ultimately become an interesting alternative to MRI-based treatment planning.

Strengths of our study can be found within the evaluated data set, because it comprised information on two prospective patient cohorts containing 24 patients. The treatment of the included patients covered different routes of needle insertion, which, to the best of our knowledge, have not yet been studied in this scientific context. Another advantage for this investigation is the high number of inserted needles

( $n = 188$ ). In addition, TRUS and MRI were performed in close temporal and local proximity to avoid applicator or needle movement between the two imaging modalities.

Limitations also arise in imaging, especially in the use of static TRUS images for comparison to MRI, and generally in the retrospective manner of this evaluation. Due to the conduct of the comparison by one observer, no statement can be made about interobserver variability. Furthermore, patient selection was limited to patients suitable for TRUS. Different needle materials should be compared in future studies to evaluate possible improvements in resolution on TRUS.

## Conclusion

Most of the needles were visible with 3D-TRUS (79%). Straight needles were better detectable than oblique needles (87% vs. 51%). Detectability was impaired by insufficient rotation angle of the TRUS probe, poor image quality or anatomic variation. Assessment of applicator geometry was comparable between MRI and TRUS. Needles show a rather indistinct signal on TRUS. It is therefore worth investigating online detection with a standardized imaging protocol in combination with needle tracking with the aim of developing real time needle guidance and online treatment planning.

## Declaration of competing interest

The department of radiation oncology at the Medical University of Vienna received payments from Elekta AB, Sweden for providing a brachytherapy workshop. NN, AS, CK, MS, and JK received honoraria for educational events from Elekta AB, Sweden. The work of ACMIT (represented by GK) was co-financed by funding in the framework of the Austrian FFG COMET program. The patent “Methods and systems for brachytherapy planning based on imaging data,” 2017 United States Patent and Trademark Office (Patent number US20170120072) was issued.

## Acknowledgments

NN was supported by the Austrian Science Fund (FWF), [project KLI695-B33](#).

## References

- [1] Pötter R, Tanderup K, Schmid MP, Jürgenliemk-Schulz I, et al. MRI-guided adaptive brachytherapy in locally advanced cervical cancer (EMBRACE-I): a multicentre prospective cohort study. *Lancet Oncol* 2021;22:538–547.
- [2] Epstein E, Testa A, Gaurilcikas A, Di Legge A, et al. Early-stage cervical cancer: tumor delineation by magnetic resonance imaging and ultrasound — A European multicenter trial. *Gynecol Oncol* 2013;128:449–453.
- [3] Schmid MP, Pötter R, Brader P, Kratochwil A, et al. Feasibility of transrectal ultrasonography for assessment of cervical cancer. *Strahlenther Onkol* 2013;189:123–128.

- [4] Pötter R, Tanderup K, Schmid MP, Jürgenliemk-Schulz I, et al. Transrectal ultrasound for image-guided adaptive brachytherapy in cervix cancer - An alternative to MRI for target definition? *Radiother Oncol* 2016;120:467–472.
- [5] Smet S, Nesvacil N, Knoth J, Sturdza A, et al. Hybrid TRUS/CT with optical tracking for target delineation in image-guided adaptive brachytherapy for cervical cancer. *Strahlenther Onkol* 2020;196:983–992.
- [6] Nesvacil N, Schmid MP, Pötter R, Kronreif G, et al. Combining transrectal ultrasound and CT for image-guided adaptive brachytherapy of cervical cancer: proof of concept. *Brachytherapy* 2016;15:839–844.
- [7] Dimopoulos JC, Petrow P, Tanderup K, Petric P, et al. Recommendations from Gynaecological (GYN) GEC-ESTRO working group (IV): basic principles and parameters for MR imaging within the frame of image based adaptive cervix cancer brachytherapy. *Radiother Oncol* 2012;103:113–122.
- [8] Rodgers JR, Bax J, Surry K, Velker V, et al. Intraoperative 360-deg three-dimensional transvaginal ultrasound during needle insertions for high-dose-rate transperineal interstitial gynecologic brachytherapy of vaginal tumors. *J Med Imaging (Bellingham)* 2019;6:025001.
- [9] Rodgers JR, Surry K, Leung E, D'Souza D, et al. Toward a 3D transrectal ultrasound system for verification of needle placement during high-dose-rate interstitial gynecologic brachytherapy. *Med Phys* 2017;44:1899–1911.
- [10] Lin Y, Shi D, Li H, Cheng G, et al. Application of transrectal ultrasound in guiding interstitial brachytherapy for advanced cervical cancer. *J Contemp Brachytherapy* 2020;12:375–382.
- [11] Poulin E, Racine E, Binnekamp D, Beaulieu L, et al. Fast, automatic, and accurate catheter reconstruction in HDR brachytherapy using an electromagnetic 3D tracking system. *Med Phys* 2015;42:1227–1232.
- [12] Yang Z, Liu Z, Jiang S, Zeng J, et al. Verification of needle guidance accuracy in pelvic phantom using registered ultrasound and MRI images for intracavitary/interstitial gynecologic brachytherapy. *J Contemp Brachytherapy* 2020;12:147–159.
- [13] Dehghan E, Bharat S, Kung C, Bonillas A, et al. EM-enhanced US-based seed detection for prostate brachytherapy. *Med Phys* 2018;45:2357–2368.
- [14] Bharat S, Kung C, Dehghan E, Ravi A, et al. Electromagnetic tracking for catheter reconstruction in ultrasound-guided high-dose-rate brachytherapy of the prostate. *Brachytherapy* 2014;13:640–650.
- [15] Boutaleb S, Racine E, Fillion O, Bonillas A, et al. Performance and suitability assessment of a real-time 3D electromagnetic needle tracking system for interstitial brachytherapy. *J Contemp Brachytherapy*;7:280–9.
- [16] Beaulieu L, Racine E, Han DY, Vigneault E, et al. Real-time electromagnetic tracking based treatment platform for high-dose-rate prostate brachytherapy: clinical workflows and end-to-end validation. *Brachytherapy* 2018;17:103–110.